Geophysical Research Letters

RESEARCH LETTER
10.1029/2018GL081501

# The Upper Stratospheric Solar Cycle Ozone Response

**W. T. Ball[1,2], E. V. Rozanov[1,2], J. Alsing[3,4], D. R. Marsh[5,6], F. Tummon[7,8], D. J. Mortlock[4,9,10], D. Kinnison[5], and J. D. Haigh[4,11]**

[1]Institute for Atmospheric and Climate Science, Swiss Federal Institute of Technology Zurich, Zurich, Switzerland, [2]Physikalisch-Meteorologisches Observatorium Davos World Radiation Centre, Davos Dorf, Switzerland, [3]Center for Computational Astrophysics, Flatiron Institute, New York, NY, USA, [4]Physics Department, Blackett Laboratory, Imperial College London, London, UK, [5]National Center for Atmospheric Research, Boulder, CO, USA, [6]School of Physics and Astronomy, University of Leeds, Leeds, UK, [7]Biosciences, Fisheries, and Economy Department, University of Tromso, Tromso, Norway, [8]Federal Office of Meteorology and Climatology MeteoSwiss, Payerne, Switzerland, [9]Department of Mathematics, Imperial College London, London, UK, [10]Department of Astronomy, Stockholm University, Stockholm, Sweden, [11]Grantham Institute – Climate Change and the Environment, Imperial College London, London, UK

**Key Points:**
- We present an assessment of upper stratospheric solar cycle (SC) ozone signals in artifact-corrected composite data sets covering 1985–2016
- The SC has a U-shaped spatial structure with peaks at ∼2 hPa (midlatitudes) and 5–10 hPa (tropics), a result of seasonal variability
- We recommend the BASIC$_{v2}$ ozone composite for chemistry climate model evaluations in the upper stratosphere

**Supporting Information:**
- Supporting Information S1
- Figure S1
- Figure S2
- Figure S3
- Figure S4
- Figure S5

**Correspondence to:**
W. T. Ball,
william.ball@env.ethz.ch

**Citation:**
Ball, W. T., Rozanov, E., Alsing, J. A., Marsh, D. R., Tummon, F., Mortlock, D. J., et al. (2019). The upper stratospheric solar cycle ozone response. *Geophysical Research Letters*, *46*, 1831–1841. https://doi.org/10.1029/2018GL081501

Received 4 DEC 2018
Accepted 27 JAN 2019
Accepted article online 31 JAN 2019
Published online 10 FEB 2019



**Abstract** The solar cycle (SC) stratospheric ozone response is thought to influence surface weather and climate. To understand the chain of processes and ensure climate models adequately represent them, it is important to detect and quantify an accurate SC ozone response from observations. Chemistry climate models (CCMs) and observations display a range of upper stratosphere (1–10 hPa) zonally averaged spatial responses; this and the recommended data set for comparison remains disputed. Recent data-merging advancements have led to more robust observational data. Using these data, we show that the observed SC signal exhibits an upper stratosphere U-shaped spatial structure with lobes emanating from the tropics (5–10 hPa) to high altitudes at midlatitudes (1–3 hPa). We confirm this using two independent chemistry climate models in specified dynamics mode and an idealized timeslice experiment. We recommend the BASIC$_{v2}$ ozone composite to best represent historical upper stratospheric solar variability, and that those based on SBUV alone should not be used.

**Plain Language Summary** Changes in the output of the Sun are thought to influence surface weather and climate through a set of processes initiated by the enhancement of upper stratosphere (32–48 km) ozone. In order to understand and assess the solar impact on the climate system, it is important that models reproduce the observed solar signal. However, the recommended data set for comparison with climate models remains disputed. We use newly improved observed ozone composites to determine both why there is disagreement between composites and which is most likely to be correct. We find that artifact-corrected composites represent the response better than those based on SBUV data alone. Further, we identify a U-shaped spatial structure with lobes emanating from the tropics to high altitudes at midlatitudes. An idealized chemistry climate model experiment and simulations considering historical meteorological conditions both support this conclusion. The results are of benefit to satellite-instrument scientists and to those engaged in atmospheric and climate research using both observations and climate models. The results will be important for assessing the solar signal in currently active and future assessments of chemistry climate models (e.g., Chemistry-Climate Model Initiative). We recommend the BASIC$_{v2}$ ozone composite to best represent historical upper stratospheric variability.

## 1. Introduction

The Sun's output varies on multiple timescales that directly affect the Earth's energy budget (Wild et al., 2013). Given that combined records of satellite observations are short (∼40 years), the most useful timescale for assessing the climate response is the 11-year solar cycle (SC), whereby the total solar irradiance varies by ∼0.1% (Kopp, 2016), influencing Earth's global surface temperatures by ∼0.08 K (Misios et al., 2016). Up to 60% of SC total solar irradiance variability is in the ultraviolet (<400 nm; Ermolli et al., 2013), which is absorbed by ozone in the Earth's stratosphere (Haigh, 1994). At solar maximum, heating and photolysis rates at tropical latitudes are enhanced, and the increase in the equator-to-pole temperature gradient is thought to modify stratospheric winter-hemispheric zonal winds and influence regional surface climate (Gray et al., 2010; Kodera & Kuroda, 2002).

However, the exact mechanisms remain poorly understood, because the observational record is short and few climate models incorporate all the processes thought required (Hood et al., 2015), i.e., a well-resolved stratosphere, accurate photolysis and heating schemes, and coupled interactive ozone chemistry. Of the ~40 CMIP5 models (Mitchell et al., 2015), only three were considered sufficiently complex to transmit the signal from the stratosphere to the surface (Figure 4 of Hood et al., 2015); eight were recently considered by Maycock et al. (2018) within the Chemistry-Climate Model Initiative (CCMI). Since stratospheric ozone is a critical starting point for a surface response, the observed SC ozone response represents an important constraint and test for climate models. Climate models that fail to represent a realistic SC ozone response are arguably unlikely to reproduce a realistic surface impact.

SC signals estimated from different observations show varying zonally averaged spatial structures and magntudes (Austin et al., 2008; Dhomse et al., 2016; Maycock et al., 2016; Soukharev & Hood, 2006). The suggested reasons include different period length and date range (Chiodo et al., 2014; Kuchar et al., 2017); data sampling and instrument-type (Hood et al., 2015; Soukharev & Hood, 2006); unit conversion between volume mixing ratio (vmr) and number density (Ball et al., 2017; Damadeo et al., 2014; Maycock et al., 2016); instrumental drifts (Li et al., 2016); artifacts in merged composites (Ball et al., 2017; Harris et al., 2015); and regression model setup, and proxies used, in the analysis (Ball et al., 2016; Chiodo et al., 2014; Marsh & Garcia, 2007; Kuchar et al., 2017). Inferring the SC from observations given these concerns is therefore challenging.

The estimated SC ozone signal also depends on the chosen data set. For example, the "Bodeker" ozone composite (Bodeker et al., 2013; Hassler et al., 2008) shows a single, broad peak in the (sub)tropical upper stratosphere (~3 hPa) as shown by Maycock et al. (2018); some CCMs display similar responses, while others display two midlatitude lobes (within ~10–2 hPa) that are sometimes connected through a tropical peak to form a U-shaped structure (Austin et al., 2008; Damadeo et al., 2014; Dhomse et al., 2011; Hood et al., 2015; Maycock et al., 2016; Sekiyama et al., 2012). The range of different SC ozone response magnitudes and zonally averaged spatial structures in models indicate that processes may be missing or misrepresented in the CCMs. Maycock et al. (2016) evaluated multiple ozone composites that showed different responses and recommended SBUVMOD v8.6 (hereafter, $SBUV_{NASA}$) as an observational reference, but clear evidence was not provided to support this choice and, consequently, identify the SC ozone response to use as a reference. Here we demonstrate that recent improvements in methods to account for data artifacts lead to more robust estimates of observed SC ozone variability for evaluating historical climate model runs. Our aim is to demonstrate which ozone data sets are reliable and hence appropriate for inclusion in future analyses.

## 2. BASIC Observational Composites

Multiple composites exist that combine ozone satellite observations into long, continuous data sets (Steinbrecht et al., 2017; Tummon et al., 2015), but these contain artifacts that can alias into the SC estimate if a standard multiple linear regression (MLR) analysis is adopted (Ball et al., 2017; Maycock et al., 2016). Artifacts are artificial variability from instrumental drifts, biases, unit conversion, sampling, and the composite-merging procedure (Ball et al., 2017, 2018; Harris et al., 2015).

Ball et al. (2017) developed the BAyeSian Integrated and Consolidated (BASIC) methodology to combine multiple composites into a single data set; BASIC was specifically developed to remove artifacts where possible or otherwise reduce their impact. The World Climate Research Program (WCRP) Stratosphere-troposphere Process and their Role in Climate (SPARC) Long-term Ozone Trends and Uncertainties in the Stratosphere (LOTUS) activity recently assessed all available ozone composites and considered BASIC to be more robust to the effect of such outliers (Petropavlovskikh et al., 2019). The BASIC approach is further described in supporting information S1. We consider four BASIC composites; the dependencies of instruments and composites that form the BASIC composites are shown and referenced in Figure S1 (Ball et al., 2018; 2017; Bourassa et al., 2017; Davis et al., 2016; Froidevaux et al., 2015; Frith et al., 2017; Petropavlovskikh et al., 2019; Sofieva et al., 2017).

## 3. Chemistry Climate Model Simulations

CCMs need to show similar variability as observations on all timescales to compare like with like. Simulations of the CCMs SOCOL (Stenke et al., 2013) and WACCM (Marsh et al., 2013) are used here to compare with the BASIC observations, which requires that chemically and dynamically driven variability is as close to

the real world as possible so that MLR analysis captures the same variability in CCMs as in the observations. Thus, for the first experiment setup we considered the two models in specified dynamics (SD) mode as in Ball et al. (2018) with CCMI-1 boundary conditions (Morgenstern et al., 2017). SD constrains CCM dynamics using temperature, wind field, and surface pressure meteorology from reanalysis to reduce CCM-specific internal variability and reproduce historical changes, while chemistry can evolve freely. SOCOL-SD (1980–2015) and WACCM-SD (1979–2014) use ERA-Interim (Dee et al., 2011) and MERRA-1 (Rienecker et al., 2011) reanalysis, respectively, and are independent (see supporting information S1 for SD-CCM specific details).

A second experimental setup was designed to reduce internal variability and isolate better the solar signal in a free-running model to ascertain if the observed zonally averaged spatial structure is robust. To do this, we perform a 10-member ensemble of timeslice experiments with free-running SOCOL, that is, without reanalysis constraints, using the SATIRE-S (Yeo et al., 2014) solar irradiance model (CCMI-1 recommends, and SD-CCMs here use, NRLSSI-1; Lean et al., 2005). SOCOL is spun-up for 10 years with constant 2008/2009 solar minimum conditions and repeating year 2000 boundary condition climatology (e.g., sea ice, sea surface temperature, greenhouse gases, and ozone depleting substances), after which solar irradiance is stepped up to constant, early-2002 solar maximum conditions for 2 years; we only consider the second year to allow for readjustments to the new solar conditions. The quasi-biennial oscillation (QBO) was switched off in this test to eliminate bias toward easterly or westerly phases (Labitzke & van Loon, 1995), so only weak easterly winds persist; this is an acceptable simplification given our focus on the photo-chemically controlled nonpolar upper stratosphere (1–10 hPa).

## 4. Multiple Linear Regression Analysis

We apply MLR as in Ball et al. (2017), except we apply the Bremen Mg II index instead of 30-cm radio flux (Dudok de Wit et al., 2014). See supporting information S1 for MLR details.

## 5. Results and Discussion

### 5.1. Equatorial Profile Ozone Changes

We begin by putting the new results in the context of previous work. Figure 1a reproduces the Soukharev and Hood (2006) (SH06) equatorial SBUV v8 (black), SAGE-II v6.2 (gray), and HALOE v19 (light-gray) profiles for periods ending in 2003; their average form another often-used reference (Austin et al., 2008) (AEA08; not shown). Since SH06 and AEA08, SAGE-II v7.0 was released (Damadeo et al., 2014), and SBUV updated to v8.6 (Frith et al., 2014, 2017; McPeters et al., 2013); these updates are included in the BASIC composites (colored profiles). It was demonstrated that conversion of SAGE-II v6.2 from number density to vmr using NCEP reanalysis temperatures led to an early trend in 1985 to 1991 that would alias, and erroneously enhance, the solar signal there (Damadeo et al., 2014, 2018; Dhomse et al., 2016; Maycock et al., 2016; Remsberg, 2014); SAGE-II v7.0 uses MERRA and does not display that behavior.

$BASIC_{SG}$ and $BASIC_{nden}$ (blue and turquoise lines, respectively), containing SAGE-II v7.0 that dominates the data in these composites for the ~1985–2003 period, show a single peak response close to 32 km (10 hPa), with $BASIC_{nden}$ displaying a slightly larger, lower peak; conversely, at this altitude the three SH06 profiles are at a minimum. The Bodeker profile (gray, dashed line) from Maycock et al. (2018) shows a similar structure to SH06 SAGE-II; this is expected since the product also contains SAGE-II v6.2. $BASIC_{SG}$ and $BASIC_{nden}$ differ from the SH06 SAGE-II profile, especially above 37 km where SAGE-II v6.2 shows a larger SC response than v7.0 (Dhomse et al., 2016; Maycock et al., 2016); HALOE does not display the same large peak at 45–50 km and is in approximate agreement with $BASIC_{SG}$, which contains HALOE, and $BASIC_{nden}$; both BASIC composites contain SAGE-II v7.0. The changes since SH06 indicate that earlier estimates may not be robust. The new composites should reflect improved data, and composites containing SAGE-II v6.2 should not be used, for example, as SH06 was in the recent CMIP5 comparative study (Hood et al., 2015).

In Figure 1a the updated $SBUV_{NASA}$ composite (yellow) shows a different equatorial structure to SBUV of SH06, with negative mean values at ~40 km exceeding the SH06 SBUV uncertainty; the inclusion of the 1979–1984 period has little impact on the profile (dotted, yellow). $BASIC_{SBUV}$ and $SBUV_{NASA}$ differ little within uncertainties, except near between 32–42 km. The reduced negative mean profile of $BASIC_{SBUV}$ supports the results of Li et al. (2016) who reported that the negative SBUV profile between 2 and 10 hPa (32–42 km) was due to a morning/afternoon observation asymmetry from satellite drift. These types of artifacts

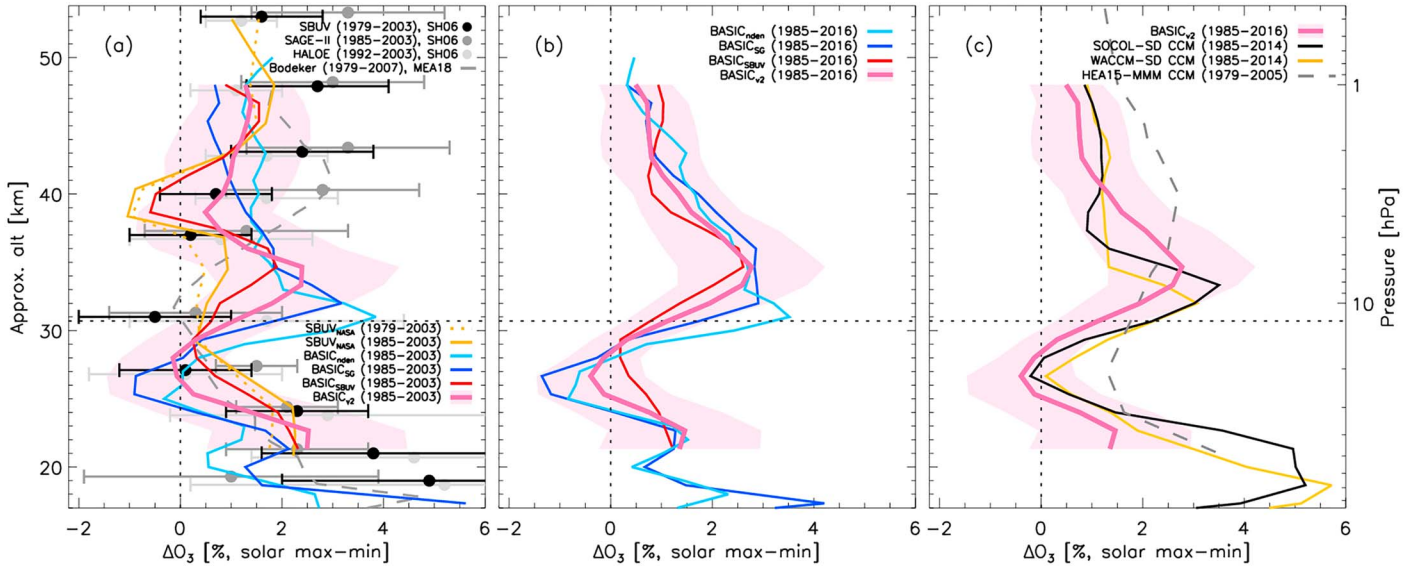


**Figure 1.** Equatorial (25° S–25° N) solar cycle ozone responses: (a) for periods considered by Soukharev and Hood (2006) (SH06), as well as the Bodeker ozone composite profile from Maycock et al. (2018) (MEA18, dashed gray; 30° S–30° N); (b) BASIC composites for 1985–2016; (c) BASIC$_{v2}$ as in (b) with the mean of three-CCMs from Hood et al. (2015) (HEA15) and SOCOL-SD and WACCM-SD CCMs. The period for each data set is given in the legends. Uncertainties are 2$\sigma$ for BASIC$_{v2}$ (shading) and SH06 (bars) only; mean profiles for all others. Multiple linear regression used the Mg-II solar proxy for an equivalent of 100 solar flux units of the 10.7-cm radio flux.

are partially accounted for using BASIC (Ball et al., 2017), including satellite changes that introduce jumps in 1994/1995 (Figures 2 and 7 in Ball et al., 2017). However, since both SBUV$_{NASA}$ and SBUV$_{NOAA}$ contain similar artifacts, the BASIC approach cannot remove features common to both composites, as there is no additional information to discriminate. The addition of SWOOSH and GOZCARDS to both SBUV composites in BASIC$_{v2}$ allows this to be addressed, leading to a profile that peaks at ~33–35 km (~7 hPa) and no negative response near 40 km. The implication is that composites containing only SBUV data should not be used to assess the SC response here.

The addition of 13 more years of data used in the MLR (shown in Figure 1b) does little to change the location of the BASIC$_{v2}$ peak and leads to a convergence of all BASIC composites to a peak response near 34 km (7 hPa); the anomalous additional peak in BASIC$_{nden}$ remains at 31 km, but the broad structure is very similar to all other BASIC composites. For context with CCMs, in Figure 1c, the mean of the three selected CCM profiles from HEA15 (one of which is WACCM in free-running mode) shows a single, broad peak at ~3 hPa, 5 km higher; BASIC$_{v2}$ is replotted from panel b. WACCM-SD and SOCOL-SD both show peaks close to but slightly lower than BASIC$_{v2}$ (10 and 8 hPa, respectively). The higher HEA15-CCM peak, similar to that of eight CCMI CCMs in Maycock et al. (2018), is in agreement with SH06, AEA08, and the Bodeker data set from Maycock et al. (2018), but again, these all employ SAGE-II v6.2 known to induce an artificially large SC response in the upper stratosphere (Damadeo et al., 2014; Maycock et al., 2016). The revised and updated composites, corrected through the BASIC method, all suggest a lower equatorial peak and are supported by historically accurate reconstructions (SD-CCMs).

### 5.2. Zonally Averaged Spatially Resolved SC Response

In Figure 2, we expand our analysis to spatially resolved, zonally averaged SC responses in the four BASIC composites; we consider the 1985–2014 period for consistency with the SD-CCMs (Figure S2 shows little change if considering 1985–2016). BASIC$_{SG}$, BASIC$_{nden}$, and BASIC$_{v2}$ show similar responses: a U-shaped spatial structure with maxima located at ~45°S and ~45°N near 1.5–3 hPa and ~7–10 hPa in the (sub)tropics. BASIC$_{SBUV}$ does not show this structure, although there is an isolated peak close to 1 hPa in the Southern Hemisphere (SH), and tropical minima near 3 hPa are present in all BASIC composites.

In the absence of other information, there is no way to assess which spatial structure is correct between independent observations, especially since SC estimates can be biased by residual variability not captured by the regression model. Therefore, fair comparisons of CCMs with observations require simulations have similar unmodeled variance as the real-world atmosphere. Since SD-CCMs are forced with historical vari-

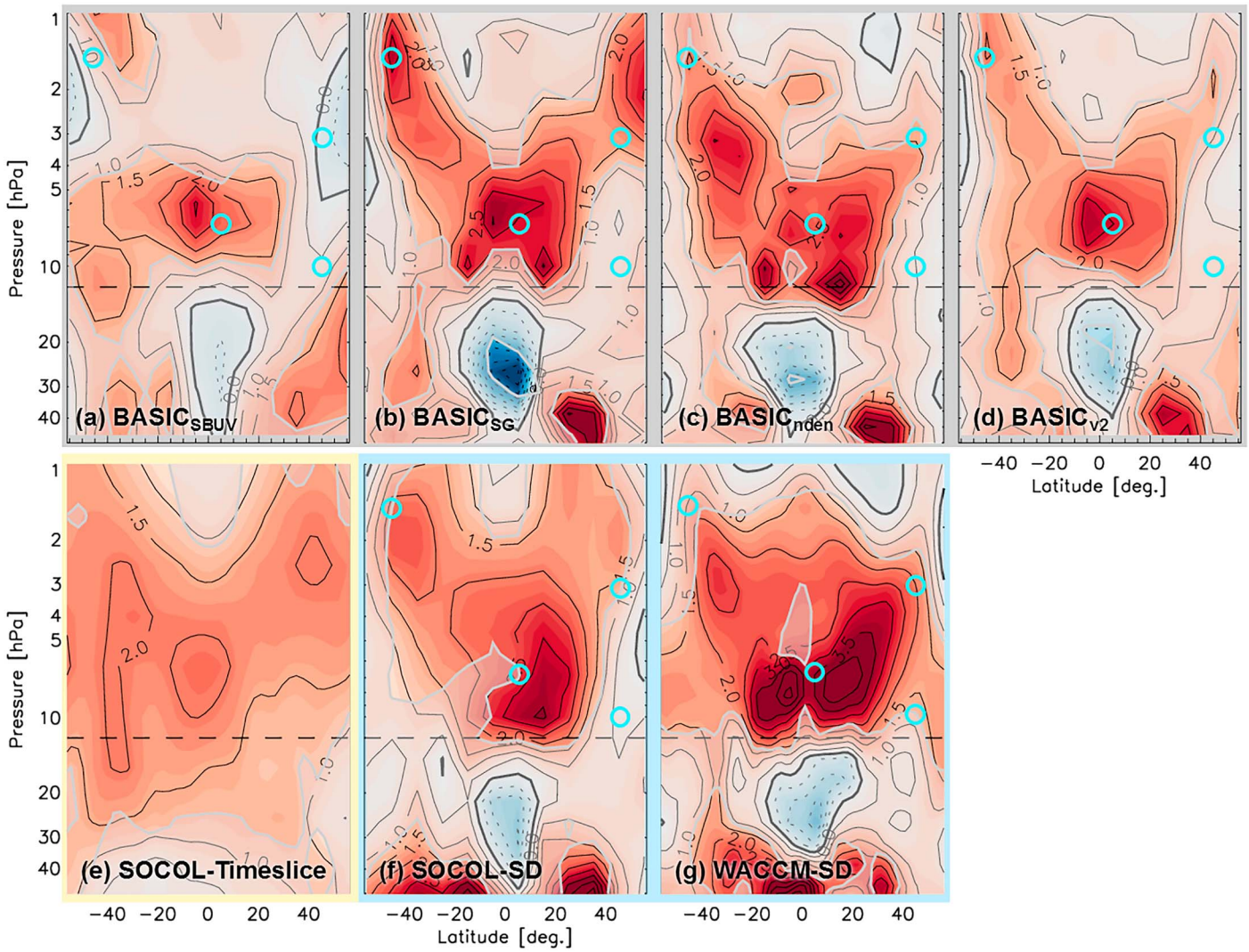


**Figure 2.** The latitude-pressure solar cycle ozone response (%) for the period 1985–2014 for four BASIC ozone composites (a–d, upper row) and two CCMs in specified dynamics mode (f–g, lower row); the SOCOL timeslice is shown in the lower left (e). Gray contours and shading represent where significance is less than $2\sigma$; blue dots represent the locations considered in Figure 4. BASIC$_{nden}$ is on geometric-altitude coordinates rescaled assuming a linear relationship with the $\log_{10}$[pressure] such that 16–48 km maps linearly to 100–1 hPa. The timeslice response is calculated from two sets of 10 ensemble runs with solar minimum (2008/2009) and solar maximum (2001/2002) conditions using the SOCOL CCM.

ability (reanalysis), they should provide a measure of data-independence to compare with observations (Ball et al., 2016; 2018), and evidence for which ozone data set is likely to be accurate irrespective of whether the estimated solar signal magnitude is correct.

Figure 2 shows that the SC estimates from SOCOL-SD and WACCM-SD display an enhanced tropical peak (~5–10 hPa) compared to BASIC$_{SG}$, BASIC$_{nden}$, and BASIC$_{v2}$, but the structure is in closer agreement with these than with BASIC$_{SBUV}$; indeed, simple spatial correlations for 60° S–60° N at and above 10 hPa yield higher correlations with BASIC$_{SG}$ (0.61 for SOCOL-SD; 0.87 for WACCM-SD) and BASIC$_{v2}$ (0.73; 0.81) than BASIC$_{SBUV}$ (0.46; 0.05). There are differences between WACCM-SD and SOCOL-SD that include (i) a less significant mid-latitude upper-stratospheric peak in WACCM-SD that appears better represented by SOCOL-SD and (ii) a stronger, two-peak response in the equatorial profile at ~7–10 hPa in WACCM-SD that appears prevalent in BASIC$_{SG}$ and BASIC$_{nden}$, while SOCOL-SD has a strong but single peak in that region. It is not clear why these differences exist, but CCMs are constructed differently, and the reanalysis nudging fields in each CCM are different and have different dynamical and temperature responses (Mitchell et al., 2015) that would directly influence ozone. Nevertheless, the gross spatial structures of the two SD-CCMs show many similarities to each other and provide evidence that BASIC$_{SG}$, BASIC$_{nden}$, and BASIC$_{v2}$ more

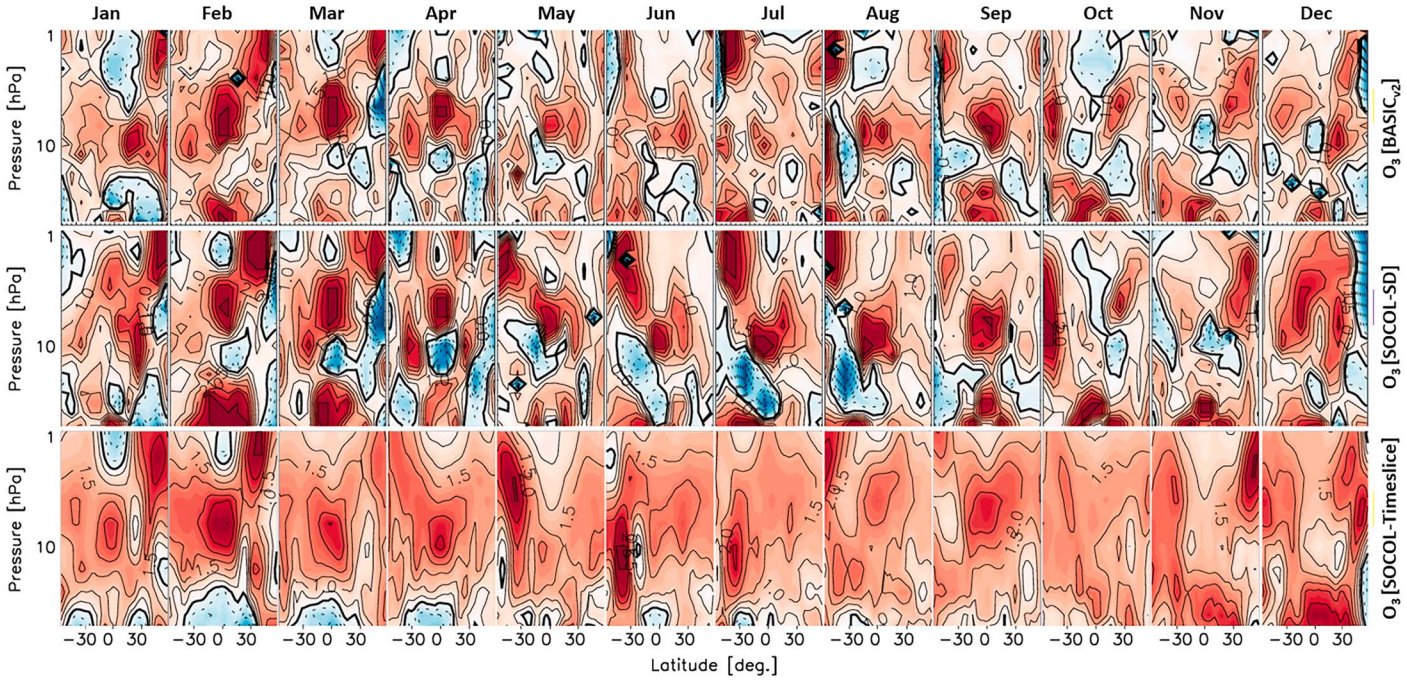


**Figure 3.** Solar cycle ozone response separated by month for (top to bottom) $BASIC_{v2}$, SOCOL-SD, and SOCOL-timeslice. Each panel ranges 60° S–60° N and 50–1 hPa.

likely represent historical SC ozone variability. This argues against the recommendation of Maycock et al. (2016) that SBUV should be considered the most appropriate for comparison of SC signals with climate models.

Some observational studies qualitatively support a U-shaped zonally averaged spatial structure, but many only display midlatitude peaks, or neither (Kyrölä et al., 2013; Maycock et al., 2016); this is similarly true for CCMs (Austin et al., 2008; Maycock et al., 2018). Indeed, free-running versions of SOCOL and WACCM (1960–2009) present only enhanced midlatitude lobes with no stratospheric tropical peak above 7 hPa (Maycock et al., 2018). Thus, the question arises: Is the U-shaped structure a reflection of the true solar ozone response, or is it an historical anomaly dependent on the specific observational period?

Figure 2e shows the solar maximum minus minimum difference from the timeslice experiments. Ozone displays a U-shaped structure, although with a reduced magnitude compared to $BASIC_{SG}$ and SOCOL-SD, and a deeper SH lobe reaching down to 15 hPa; such a deeper extension to lower altitudes in the SH is also apparent in $BASIC_{v2}$. Possible explanations for the differences include (i) the QBO is inactive; (ii) unmodeled variability aliases with regressors in the SD-CCMs or observations; and (iii) the timeslice experiments have a climate-model specific internal variability. The absence of a negative peak near 15 hPa in the timeslice analysis hints that this structure may have a relationship to the QBO, which is absent in the timeslice experiment, or that how MLR is applied may play a role in its appearance (Smith & Matthes, 2008). Indeed, qualitatively this agrees with Figure 8 of Chiodo et al. (2014) where the absence of a QBO in the model experiments leads to a small upward shift in the peak while the negative response disappears lower down; this result is consistent with the idealized timeslice experiment. Overall, the midlatitude peaks/lobes appear consistent, with some evidence for a tropical peak near 5–10 hPa. This implies that the U-shaped structure, with a peak near 5–10 hPa is not just a result of unmodeled variability during the observational era (since 1979), but a real structure in the response of stratospheric ozone to SC variability.

The reason for the U-shaped structure is revealed in Figure 3 where regression has been performed separately for each month; each panel displays the 60° S–60° N, 1–50 hPa SC ozone response for $BASIC_{v2}$, SOCOL-SD CCM, and SOCOL timeslice. Clear positive peaks in the timeslice simulations are in qualitative agreement in most months with SOCOL-SD or $BASIC_{v2}$. High-latitude upper stratosphere maxima become particularly pronounced during winter in both hemispheres, for example, November to March in the Northern Hemisphere (NH) and July to September in the SH. This suggests that the mechanism for increased

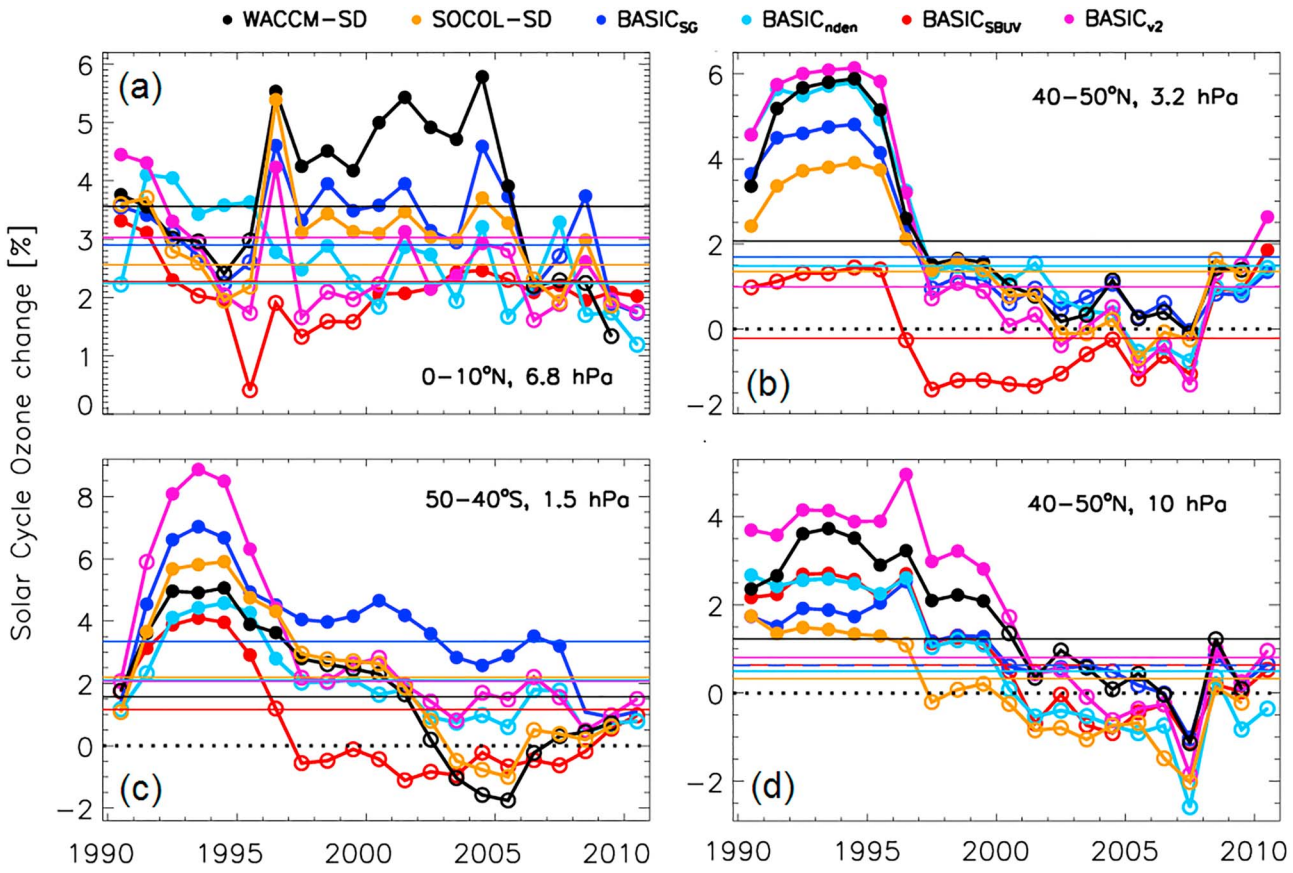


**Figure 4.** The evolution of the multiple linear regression-estimated solar cycle ozone signal (%) using 11-year windows centered on the dates at each dot for four latitude-pressure locations (see labels). These locations are highlighted as light-blue circles in Figure 2. Horizontal colored lines represent the 1985–2014 mean results from Figure 2. If statistically significant ($2\sigma$) the circle is solid; otherwise, it is open.

ozone could be the seasonal dependence of the meridional Brewer Dobson circulation and/or enhanced tropical upwelling; further investigation is required. The equatorial peak is present in both winter periods, though for longer during SH winter. While the peaks in the timeslice experiment are almost always apparent in SOCOL-SD and BASIC$_{v2}$, except in July, the alternative is not true; for example, high-altitude, SH peaks in June and July appear to be absent in the timeslice experiment. Further, the QBO appears to interfere with the height and extent of the tropical peak consistently from February to June, and no negative response is seen in the timeslice without a QBO, but whether this is due to a regression or dynamical aspect remains an open question (Chiodo et al., 2014; Smith & Matthes, 2008). In most months, the structure and magnitude of the SC ozone response agree well between SOCOL-SD and BASIC$_{v2}$, further supporting the robustness of the spatial structure.

In summary, there is agreement between timeslice, SOCOL-SD CCM, and BASIC$_{v2}$ in monthly variability. Given the average of the monthly timeslice results lead to a U-shaped structure (not shown), this provides evidence that the structure is a result of seasonal variations in the SC; the physical cause will be the focus of a follow-up study.

### 5.3. Why SBUV Does Not Display the U-shaped Response

The time-dependent SC signal demonstrated in Figure 1 (e.g., BASIC$_{SBUV}$) provides a way to assess which ozone composites are better for estimating the SC response. Since SD-CCMs and observations should contain the same historical ozone variability, given that the same regression model, the magnitude should evolve similarly provided that CCM photochemistry is correct. Thus, we select four locations (blue circles, Figure 2) in all data sets. MLR is applied without a trend-term to a sliding 11-year regression-window, first centered on 1990, covering 1985–1995. This is repeated for 1991, and so on until 2010 (2009 for SD-CCMs), and plotted in Figure 4; the 1985–2014 values in Figure 2 are shown as horizontal lines. The inclusion of years following

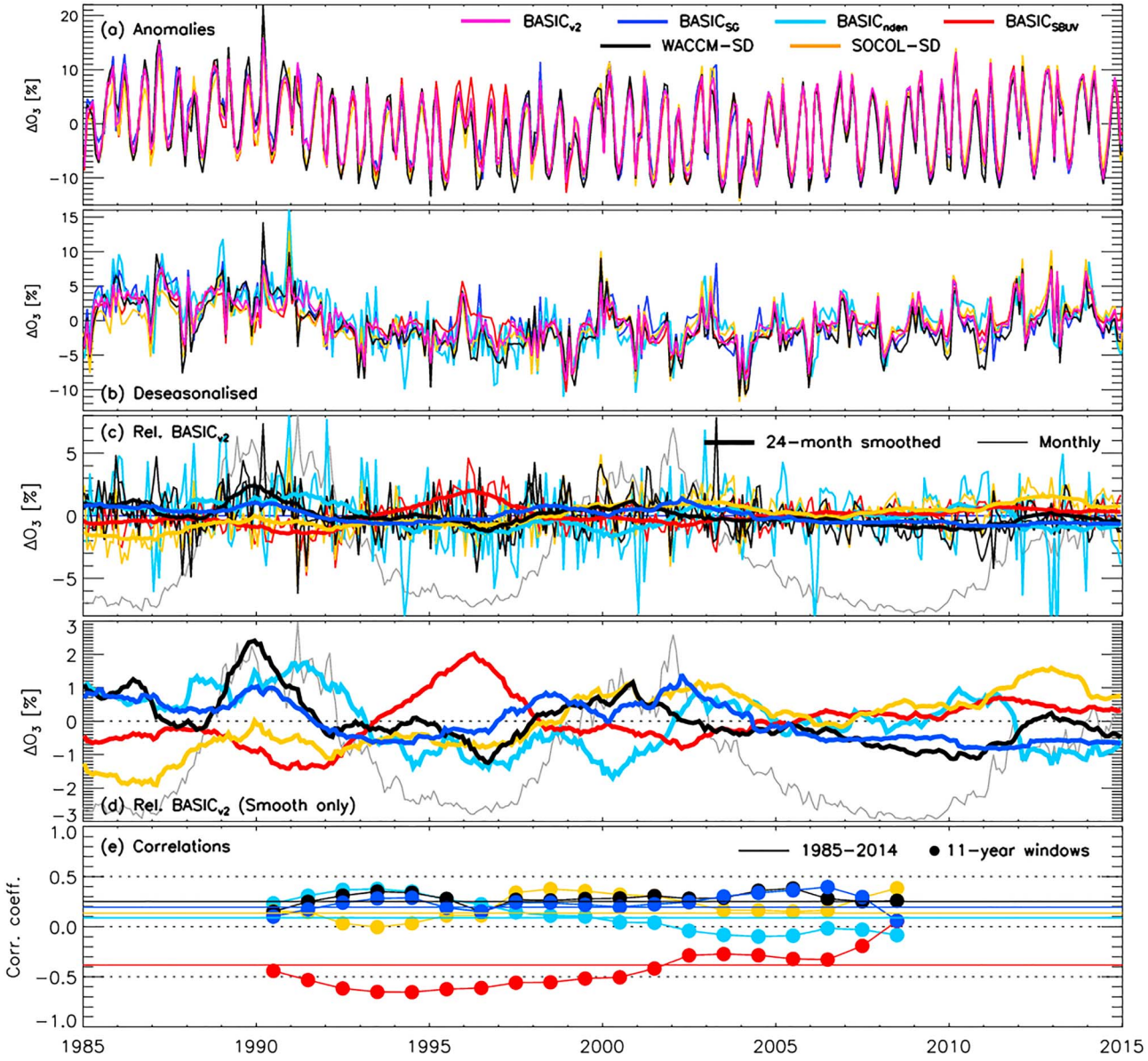


**Figure 5.** Ozone timeseries at 3.2 hPa (~40 km) and 40–50° N: (a) monthly anomalies; (b) deseasonalised anomalies; (c) deseasonalized anomalies relative to BASIC$_{v2}$ with 24-month boxcar smoothed time series (thick lines), and the unitless Mg-II solar proxy plotted in the background; (d) the smoothed timeseries and Mg-II proxy (gray) from (c); (e) the correlation coefficient of the Mg-II proxy with the monthly ozone anomalies of each data set relative to BASIC$_{v2}$ in (c) in 11-year windows centered on each dot, along with the 1985–2014 correlation coefficient (solid horizontal lines).

the two major eruptions (Figure S3), or if a longer 22-year window is adopted (Figure S4), has little impact on the following discussion.

Figure 4 reveals that the MLR-estimated solar signal depends on the period and so can evolve over time. We cannot currently ascribe this as a real (nonlinear) evolution in the ozone response, or quantify aliasing between regressors and/or unmodeled variability. The notably rapid change around 1997/1998 in all data sets (Figures 4b and 4c) is possibly due to aliasing between the volcanic and solar proxies (Chiodo et al., 2014; Kuchar et al., 2017), but only after Mt. Pinatubo (1994–2004 onward) when background level of the stratospheric aerosol optical depth (SAOD) correlate with the solar proxy (Figure S5a); the QBO shows little evolving solar correlation ($r < \pm 0.2$; Figure S5b), while ENSO3.4 does display some ($r < \pm 0.3$; Figure S5c). However, it is difficult to disentangle the simultaneous cross-correlation between multiple proxies (see Figure 7 of Kuchar et al., 2017). Figure 4d provides an example where all observations and CCMs display similar behavior, and BASIC$_{SBUV}$ does not show any anomalous behavior compared to the others. However,

in the other three panels (Figures 4a–4c) near the three lobes that form the U-shaped structure $BASIC_{SBUV}$ is the lowest of the pack and displays a different evolution.

In particular, in Figure 4b, at 40–50° N and 3.2 hPa near the NH peak, all data sets evolve with similar absolute levels and temporal changes except $BASIC_{SBUV}$, which is more strongly affected around 1996. Comparing the time series here reveals why. Figures 5a and 5b show the ozone anomalies and deseasonalized time series at 3.2 hPa and 40–50° N. We subtract $BASIC_{v2}$ from all composites in Figure 5c to give relative changes with smoothed time series, made clearer in Figure 5d, along with the solar proxy. In Figure 5e, the 11-year window correlation coefficient of the monthly solar proxy with $BASIC_{v2}$-relative time series from Figure 5d reveals $BASIC_{SBUV}$ has a consistently negative correlation that peaks around 2001/2002: during this period, the smoothed time series anticorrelate with the solar proxy (Figure 5d) and reduce the MLR-estimated solar signal. The anticorrelation results from the aforementioned SBUV satellite drift and switch (Figure 7 of Ball et al., 2017), confirming the effect as a composite artifact. This reinforces the conclusion that current SBUV-composites should not be used to assess the SC signal.

Overall, we find that it is likely that SBUV does not display the U-shaped structure due to the presence of artifacts in the time series. Further, the evolution of the SC response in $BASIC_{SG}$, $BASIC_{nden}$, $BASIC_{v2}$, and the SD-CCMs agree reasonably well. We conclude that BASIC composites other than $BASIC_{SBUV}$ form a viable reference for evaluation of climate models over the satellite period.

## 6. Summary and Conclusions

We present results from new ozone composites formed using Bayesian algorithms designed to account for artifacts that bias the SC ozone response in the upper stratosphere (1–10 hPa) estimated using MLR. We find that SBUV-based composites differ in the zonally averaged response compared to the other composites as a result of artifacts in SBUV composites that anticorrelate with the solar proxy to reduce the attributed signal. We show that a U-shaped spatial structure in BASIC composites containing SAGE-II v7.0 is a likely feature that forms from seasonal changes. This is evidenced by (i) improved, artifact-corrected ozone composites; (ii) agreement with two independent SD-CCMs; and (iii) an idealized, timeslice experiment. The U-shaped structure provides a focus for future studies comparing observational and climate model results.

Currently, we cannot infer a "correct" time-independent solar signal due to its time evolution; more observations are needed for a confident result (Chiodo et al., 2014; Kuchar et al., 2017). Indeed, we question the validity of detecting a true solar signal using linear regression models when the ozone response is generally accepted to be nonlinear (Labitzke & van Loon, 1988; Roy & Haigh, 2011). However, the results presented still provide a measure to assess the consistency of the SC response between observations and simulations, as long as MLR is used consistently and unmodeled residual variability alias with proxies in a similar way. Missing processes or CCM-dependent internal variability may further interfere. Consideration of this topic is an aim within the SPARC SOLARIS-HEPPA initiative. Our results make clear that composites containing SAGE-II v6.2, or only SBUV data, should not be considered without clearly stating the associated caveats. Despite these concerns, we recommend $BASIC_{v2}$ for estimating the upper stratospheric solar signal *given the assumptions of the regression model used to extract it and the period considered* due to good agreement with the CCM experiments while including both SBUV and SAGE-II v7.0.

**Acknowledgments**
We thank A. Laeng for use of the unpublished SAGE-II-OSIRIS-OMPS (Petropavlovskikh et al., 2019) data in the construction of $BASIC_{nden}$, and the SPARC LOTUS working group for inspiring its construction, and comments and feedback. We also thank J. Stähelin for useful input on the manuscript. Thanks for fruitful discussions in the framework of WG3 of SPARC SOLARIS-HEPPA. W. T. B. and E. V. R. were funded by SNSF project 163206 (SIMA). F. T. was funded by SNSF Grant 20F121_138017. NCAR is sponsored by the National Science Foundation. Computing resources were provided by the Climate Simulation Laboratory at NCAR's Computational and Information Systems Laboratory (CISL), sponsored by the National Science Foundation and other agencies. The CCMI model simulations from WACCM can be requested at https://www.earthsystemgrid.org/search.html? Project=CCMI1. BASIC data products can be found at https://data.mendeley.com/datasets/2mgx2xzzpk/2. We thank two reviewers, R. Thieblemont and one anonymous, for their useful suggestions that improved the paper.

## References

Austin, J., Tourpali, K., Rozanov, E., Akiyoshi, H., Bekki, S., Bodeker, G., et al. (2008). Coupled chemistry climate model simulations of the solar cycle in ozone and temperature. *Journal of Geophysical Research*, *113*, D11306. https://doi.org/10.1029/2007JD009391

Ball, W. T., Alsing, J., Mortlock, D. J., Rozanov, E. V., Tummon, F., & Haigh, J. D. (2017). Reconciling differences in stratospheric ozone composites. *Atmospheric Chemistry & Physics*, *17*, 12,269–12,302.

Ball, W. T., Alsing, J., Mortlock, D. J., Staehelin, J., Haigh, J. D., Peter, T., et al. (2018). Evidence for a continuous decline in lower stratospheric ozone offsetting ozone layer recovery. *Atmospheric Chemistry & Physics*, *18*, 1379–1394.

Ball, W. T., Haigh, J. D., Rozanov, E. V., Kuchar, A., Sukhodolov, T., Tummon, F., et al. (2016). High solar cycle spectral variations inconsistent with stratospheric ozone observations. *Nature Geoscience*, *9*, 206–209.

Ball, W. T., Kuchař, A., Rozanov, E. V., Staehelin, J., Tummon, F., Smith, A. K., et al. (2016). An upper-branch Brewer-Dobson circulation index for attribution of stratospheric variability and improved ozone and temperature trend analysis. *Atmospheric Chemistry & Physics*, *16*, 15,485–15,500.

Bodeker, G. E., Hassler, B., Young, P. J., & Portmann, R. W. (2013). A vertically resolved, global, gap-free ozone database for assessing or constraining global climate model simulations. *Earth System Science Data*, *5*, 31–43.

Bourassa, A. E., Roth, C. Z., Zawada, D. J., Rieger, L. A., McLinden, C. A., & Degenstein, D. A. (2017). Drift corrected Odin-OSIRIS ozone product: Algorithm and updated stratospheric ozone trends. *Atmospheric Measurement Techniques Discuss*, *11*, 489–498.

Chiodo, G., Marsh, D. R., Garcia-Herrera, R., Calvo, N., & García, J. A. (2014). On the detection of the solar signal in the tropical stratosphere. *Atmospheric Chemistry & Physics*, *14*, 5251–5269.

Damadeo, R. P., Zawodny, J. M., Remsberg, E. E., & Walker, K. A. (2018). The impact of nonuniform sampling on stratospheric ozone trends derived from occultation instruments. *Atmospheric Chemistry & Physics*, *18*, 535–554.

Damadeo, R. P., Zawodny, J. M., & Thomason, L. W. (2014). Reevaluation of stratospheric ozone trends from SAGE II data using a simultaneous temporal and spatial analysis. *Atmospheric Chemistry & Physics*, *14*, 13,455–13,470.

Davis, S. M., Rosenlof, K. H., Hassler, B., Hurst, D. F., Read, W. G., Vömel, H., et al. (2016). The Stratospheric Water and Ozone Satellite Homogenized (SWOOSH) database: A long-term database for climate studies. *Earth System Science Data*, *8*, 461–490.

Dee, D. P., Uppala, S. M., Simmons, A. J., Berrisford, P., Poli, P., Kobayashi, S., et al. (2011). The ERA-Interim reanalysis: configuration and performance of the data assimilation system. *Quarterly Journal of the Royal Meteorological Society*, *137*, 553–597.

Dhomse, S. S., Chipperfield, M. P., Damadeo, R. P., Zawodny, J. M., Ball, W. T., Feng, W., et al. (2016). On the ambiguous nature of the 11 year solar cycle signal in upper stratospheric ozone. *Geophysical Research Letters*, *43*, 7241–7249. https://doi.org/10.1002/2016GL069958

Dhomse, S. S., Chipperfield, M. P., Feng, W., & Haigh, J. D. (2011). Solar response in tropical stratospheric ozone: A 3-D chemical transport model study using ERA reanalyses. *Atmospheric Chemistry & Physics*, *11*, 12,773–12,786.

Dudok de Wit, T., Bruinsma, S., & Shibasaki, K. (2014). Synoptic radio observations as proxies for upper atmosphere modelling. *Journal of Space Weather and Space Climate*, *4*(27), A06.

Ermolli, I., Matthes, K., Dudok de Wit, T., Krivova, N. A., Tourpali, K., Weber, M., et al. (2013). Recent variability of the solar spectral irradiance and its impact on climate modelling. *Atmospheric Chemistry and Physics*, *13*, 3945–3977.

Frith, S. M., Kramarova, N. A., Stolarski, R. S., McPeters, R. D., Bhartia, P. K., & Labow, G. J. (2014). Recent changes in total column ozone based on the SBUV Version 8.6 Merged Ozone Data Set. *Journal of Geophysical Research: Atmospheres*, *119*, 9735–9751. https://doi.org/10.1002/2014JD021889

Frith, S. M., Stolarski, R. S., Kramarova, N. A., & McPeters, R. D. (2017). Estimating Uncertainties in the SBUV Version 8.6 Merged Profile Ozone Dataset. *Atmospheric Chemistry and Physics Discuss*, *17*, 14695.

Froidevaux, L., Anderson, J., Wang, H.-J., Fuller, R. A., Schwartz, M. J., Santee, M. L., et al. (2015). Global OZone Chemistry And Related trace gas Data records for the Stratosphere (GOZCARDS): Methodology and sample results with a focus on HCl, $H_2O$, and $O_3$. *Atmospheric Chemistry & Physics*, *15*, 10,471–10,507.

Gray, L. J., Beer, J., Geller, M., Haigh, J. D., Lockwood, M., Matthes, K., et al. (2010). Solar influences on climate. *Reviews of Geophysics*, *48*, RG4001. https://doi.org/10.1029/2009RG000282

Haigh, J. D. (1994). The role of stratospheric ozone in modulating the solar radiative forcing of climate. *Nature*, *370*, 544–546.

Harris, N. R. P., Hassler, B., Tummon, F., Bodeker, G. E., Hubert, D., Petropavlovskikh, I., et al. (2015). Past changes in the vertical distribution of ozone—Part 3: Analysis and interpretation of trends. *Atmospheric Chemistry & Physics*, *15*, 9965–9982.

Hassler, B., Bodeker, G. E., & Dameris, M. (2008). Technical note: A new global database of trace gases an aerosols from multiple sources of high vertical resolution measurements. *Atmospheric Chemistry & Physics*, *8*, 5403–5421.

Hood, L. L., Misios, S., Mitchell, D. M., Rozanov, E., Gray, L. J., Tourpali, K., et al. (2015). Solar signals in CMIP-5 simulations: The ozone response. *Quarterly Journal of the Royal Meteorological Society*, *141*, 2670–2689.

Kodera, K., & Kuroda, Y. (2002). Dynamical response to the solar cycle. *Journal of Geophysical Research*, *107*, 4749.

Kopp, G. (2016). Magnitudes and timescales of total solar irradiance variability. ArXiv e-prints.

Kuchar, A., Ball, W. T., Rozanov, E. V., Stenke, A., Revell, L., Miksovsky, J., et al. (2017). On the aliasing of the solar cycle in the lower stratospheric tropical temperature. *Journal of Geophysical Research: Atmospheres*, *122*, 9076–9093. https://doi.org/10.1002/2017JD026948

Kyrölä, E., Laine, M., Sofieva, V., Tamminen, J., Päivärinta, S.-M., Tukiainen, S., et al. (2013). Combined SAGE II-GOMOS ozone profile data set for 1984-2011 and trend analysis of the vertical distribution of ozone. *Atmospheric Chemistry & Physics*, *13*, 10,645–10,658.

Labitzke, K., & van Loon, H. (1988). Associations between the 11-year solar cycle, the qbo and the atmosphere. I—The troposphere and stratosphere in the Northern Hemisphere in winter. *Journal of Atmospheric and Terrestrial Physics*, *50*, 197–206.

Labitzke, K., & van Loon, H. (1995). Connection between the troposphere and stratosphere on a decadal scale. *Tellus Series A*, *47*, 275.

Lean, J., Rottman, G., Harder, J., & Kopp, G. (2005). SORCE contributions to new understanding of global change and solar variability. *Journal of Solar Physics*, *230*, 27–53.

Li, K.-F., Zhang, Q., Tung, K.-K., & Yung, Y. L. (2016). Resolving a long-standing model-observation discrepancy on ozone solar cycle response. *Earth and Space Science*, *3*, 431–440.

Marsh, D. R., & Garcia, R. R. (2007). Attribution of decadal variability in lower-stratospheric tropical ozone. *Geophysical Research Letters*, *34*, L21807. https://doi.org/10.1029/2007GL030935

Marsh, D. R., Mills, M. J., Kinnison, D. E., Lamarque, J.-F., Calvo, N., & Polvani, L. M. (2013). Climate Change from 1850 to 2005 Simulated in CESM1(WACCM). *Journal of Climate*, *26*, 7372–7391.

Maycock, A. C., Matthes, K., Tegtmeier, S., Schmidt, H., Thiéblemont, R., Hood, L., et al. (2018). The representation of solar cycle signals in stratospheric ozone part 2: Analysis of global models. *Atmospheric Chemistry and Physics*, *18*, 11,323–11,343.

Maycock, A. C., Matthes, K., Tegtmeier, S., Thiéblemont, R., & Hood, L. (2016). The representation of solar cycle signals in stratospheric ozone—Part 1: A comparison of recently updated satellite observations. *Atmospheric Chemistry & Physics*, *16*, 10,021–10,043.

McPeters, R. D., Bhartia, P. K., Haffner, D., Labow, G. J., & Flynn, L. (2013). The version 8.6 SBUV ozone data record: An overview. *Journal of Geophysical Research: Atmospheres*, *118*, 8032–8039. https://doi.org/10.1002/jgrd.50597

Misios, S., Mitchell, D. M., Gray, L. J., Tourpali, K., Matthes, K., Hood, L., et al. (2016). Solar signals in CMIP-5 simulations: Effects of atmosphere-ocean coupling. *Quarterly Journal of the Royal Meteorological Society*, *142*, 928–941.

Mitchell, D. M., Gray, L. J., Fujiwara, M., Hibino, T., Anstey, J. A., Ebisuzaki, W., et al. (2015). Signatures of naturally induced variability in the atmosphere using multiple reanalysis datasets. *Quarterly Journal of the Royal Meteorological Society*, *141*, 2011–2031.

Mitchell, D. M., Misios, S., Gray, L. J., Tourpali, K., Matthes, K., Hood, L., et al. (2015). Solar signals in CMIP-5 simulations: The stratospheric pathway. *Quarterly Journal of the Royal Meteorological Society*, *141*, 2390–2403.

Morgenstern, O., Hegglin, M. I., Rozanov, E., O'Connor, F. M., Abraham, N. L., Akiyoshi, H., et al. (2017). Review of the global models used within phase 1 of the Chemistry-Climate Model Initiative (CCMI). *Geoscientific Model Development*, *10*, 639–671.

Petropavlovskikh, I., Godin-Beekmann, S., Hubert, D., Damadeo, R., Hassler, B., & Sofieva, V. (2019). Sparc/io3c/gaw report on long-term ozone trends and uncertainties in the stratosphere. SPARC/IO3C/GAW, SPARC Report No. 9, WCRP-17/2018, GAW Report No. 241.

Remsberg, E. E. (2014). Decadal-scale responses in middle and upper stratospheric ozone from SAGE II version 7 data. *Atmospheric Chemistry and Physics*, *14*, 1039–1053.

Rienecker, M. M., Suarez, M. J., Gelaro, R., Todling, R., Bacmeister, J., Liu, E., et al. (2011). MERRA: NASA's modern-era retrospective analysis for research and applications. *Journal of Climate*, *24*, 3624–3648.

Roy, I., & Haigh, J. D. (2011). The influence of solar variability and the quasi-biennial oscillation on lower atmospheric temperatures and sea level pressure. *Atmospheric Chemistry & Physics*, *11*, 11,679–11,687.

Sekiyama, T. T., Shibata, K., Deushi, K., Kodera, K., & Lean, J. L. (2012). Stratospheric ozone variation induced by the 11-year solar cycle: Recent 22-year simulation using 3-D chemical transport model with reanalysis data. *Geophysical Research Letters*, *33*, L17812. https://doi.org/10.1029/2006GL026711

Smith, A. K., & Matthes, K. (2008). Decadal-scale periodicities in the stratosphere associated with the solar cycle and the QBO. *Journal of Geophysical Research*, *113*, D05311. https://doi.org/10.1029/2007JD009051

Sofieva, V. F., Kyrölä, E., Laine, M., Tamminen, J., Degenstein, D., Bourassa, A., et al. (2017). Merged SAGE II, Ozone_cci and OMPS ozone profiles dataset and evaluation of ozone trends in the stratosphere. *Atmospheric Chemistry and Physics*, *17*, 12,533–12,552. https://doi.org/10.5194/acp-17-12533-2017

Soukharev, B. E., & Hood, L. L. (2006). Solar cycle variation of stratospheric ozone: Multiple regression analysis of long-term satellite data sets and comparisons with models. *Journal of Geophysical Research*, *111*, D20314. https://doi.org/10.1029/2006JD007107

Steinbrecht, W., Froidevaux, L., Fuller, R., Wang, R., Anderson, J., Roth, C., et al. (2017). An update on ozone profile trends for the period 2000 to 2016. *Atmospheric Chemistry and Physics Discuss*, *2017*, 1–24.

Stenke, A., Schraner, M., Rozanov, E., Egorova, T., Luo, B., & Peter, T. (2013). The SOCOL version 3.0 chemistry-climate model: Description, evaluation, and implications from an advanced transport algorithm. *Geoscientific Model Development*, *6*, 1407–1427.

Tummon, F., Hassler, B., Harris, N. R. P., Staehelin, J., Steinbrecht, W., Anderson, J., et al. (2015). Intercomparison of vertically resolved merged satellite ozone data sets: Interannual variability and long-term trends. *Atmospheric Chemistry & Physics*, *15*, 3021–3043.

Wild, M., Folini, D., Schär, C., Loeb, N., Dutton, E. G., & König-Langlo, G. (2013). The global energy balance from a surface perspective. *Climate Dynamics*, *40*, 3107–3134.

Yeo, K. L., Krivova, N. A., Solanki, S. K., & Glassmeier, K. H. (2014). Reconstruction of total and spectral solar irradiance from 1974 to 2013 based on KPVT, SoHO/MDI, and SDO/HMI observations. *Astronomy & Astrophysics*, *570*, A85.